Summer 2019

Curbside Antenna to Vehicle Path Loss Measurements and Modeling in Three Frequency Bands

Patrick Murphy

Curbside Antenna to Vehicle Path Loss Measurements and Modeling in Three Frequency Bands

by

Patrick Murphy

Bachelor of Science
University of South Carolina, 2015

Submitted in Partial Fulfillment of the Requirements

For the Degree of Master of Science in

Electrical Engineering

College of Engineering and Computing

University of South Carolina

2019

Accepted by:

David Matolak, Director of Thesis

Mohammod Ali, Reader

Cheryl L. Addy, Vice Provost and Dean of the Graduate School

Dedication

To my Mother for her continuing support.

Acknowledgements

I would like to thank Mathew Davidson and Nozhan Hosseini for assisting me with my tests and for letting me practice my presentation with them. Dr. Ali for agreeing to be on my Defense Committee on such short notice and the helpful feedback he gave. And finally Dr. Matolak, for taking me on as his student and for all his support over the last couple years without which I would not be where I am today.

Abstract

V2V and V2I systems have been an increasingly important topic of study in recent years. Future V2I systems could involve antennas near or on the curb at intersections or on the ground along highways. To this end the curbside antenna to vehicle channel has not been studied very much. The scope of this thesis is to develop initial models for the path loss for examples of this channel. This was done through a measurement campaign where the transmitting antenna is located on the ground near the road and the receiver is in a vehicle driving towards the transmitter. The vehicle drove a distance of 100 m toward the transmitter and received power was recorded loss in route; from received power and other known link parameters, path loss was calculated. This test was done at three distinct frequencies, 700 MHz, 2.4 GHz and 5 GHz, at two different locations, rural and urban, and with two different antenna positions, inside and outside of the vehicle. A log-distance path loss model was created for each case and the path loss exponents, intercept points, and standard deviations of the path loss fit lines were tabulated. It was found that the urban location tended to have smaller path loss exponents than the rural location. The urban exponents were closer to 2, the exponent of free-space, and this result is most likely due to multipath components in the less open environment. The 5 GHz cases had the lowest path loss exponents, all near 1; this indicates significant waveguiding by the street-side buildings in the urban case at this frequency. The path loss exponents ranged from 1.1 to 3.6, and standard deviations ranged from 4.9 to 13.1 dB.

.

Table of Contents

List of Tables

List of Figures

Chapter 1. Introduction

1.1 Motivation

Vehicle-to-Vehicle (V2V) and Vehicle-to-Infrastructure (VTI) communications have been an important topic of study in recent years, and interest in creating these systems is likely to continue to grow as they become more ubiquitous [1]-[3]. These systems will be used to improve road safety and provide drivers with traffic updates to help the flow of traffic, among other applications [3]. Our focus is not on these applications, but on ensuring link quality, and for that, path loss, or wireless channel attenuation, should be well characterized. For some applications, near-ground sensors at intersections may be used to monitor traffic flow, or along a highway to measure vehicle speed, or for other services. Thus, it is of interest to characterize the channel between a near-ground sensor and a vehicle on the road.

1.2 Literature Review

When defining a radio channel there are certain characteristics that are of interest such as path loss and channel impulse response. Though the focus of this thesis is on path loss it is worth briefly describing the others and their importance in channel modeling. Path loss refers to the amount of power that is lost as the signal propagates from the transmitter to the receiver. There are several causes of path loss, including absorption and/or reflection from obstacles between transmitter and receiver, multiple receptions of the transmitted signal causing destructive interference at the receiver, and simply power loss of a signal as

it propagates. Path loss models are thus created to predict the path loss a communication system might expect in a given environment. These models can be geometric, empirical, deterministic, or stochastic in nature [4]. The channel impulse response is the channel's output when a single impulse is applied. A wireless channel can be thought of as a linear time-varying system . By measuring the output response to an impulse, we can learn what the output will be for any signal input given the system is linear time invariant (LTI) [5]; most channels are slowly time varying and hence can be considered TI for some short duration.

References [1] and [2] both discuss measurement campaigns for V2V communications in various environments. In [1], the measurements consist of wideband measurements at frequency f = 5.12 GHz, within five cities and along their highways to simulate what a "user could encounter during the course of travel." The measurements were classified into five different environments; Urban-Antenna Outside Car, Urban-Antenna Inside Car, Small City, Open Area-Low Traffic Density, and Open Area High Traffic Density. This paper found that though each environment behaved differently, the Urban-Antenna Inside Car environment was the most dispersive case. The authors of [2] focus primarily on path loss for V2V communications in four different environments; highway, rural, urban and suburban for a frequency of 5.2 GHz. They investigated several models for path loss, and estimated the path loss exponent. The path loss exponent quantifies the rate at which channel attenuation increases as a function of distance. They found the path loss exponent for the highway and urban environments to be less than 2 and found the so-called 2-ray model to provide the best fit for the rural environment. The 2-ray model represents the channel with a line-of-sight path and an earth surface reflection.

Sources [7] and [8] discuss the effects of low-height antennas on various channel properties such as path loss, standard deviation of the path loss about the linear fit, and RMS delay spread (the standard deviation of the delays weighted by their relative power) [6]. In [7] measurements were performed indoors in various LOS and NLOS locations. The measurements show that placing the antennas on or near the ground increases path loss, standard deviation, and RMS delay spread for both LOS and NLOS environments. In [8], the measurements were performed in two outdoor environments, an open field for LOS scenarios and in a forest for scenarios with large numbers of scattering objects. Both narrowband and wideband measurements were taken for frequencies of 300 MHz and 1900 MHz with link distances up to 500 m for some cases. The wideband LOS results showed that the "path loss decreases by 7-10 dB when the antenna height is increased from 0.45 to 1.65 m. The narrowband forested environments show the path loss "varies inversely to the square of the receiving antenna height."

The scope of this thesis is to investigate the low-height (curbside) antenna to vehicle channel, specifically to quantify the path loss of such a channel in several frequency bands. To our knowledge, work in the literature only investigates either V2V communication or the effects of low-height antennas, but not both. Thus, our contribution is to begin to fill this gap.

1.3 Thesis Contents

In Chapter 2 the theories for path loss models and antenna radiation patterns are reviewed. Chapter 3 describes our channel measurement test procedure, including a description of the two test environments, with a list of all test equipment and photographs of the test setup in the field. The test environments are South Beltline Blvd, and Main St.

In Chapter 4 the results of the experiment are discussed, and the attenuation is first compared to that of free space and 2-ray path loss versus distance. Average attenuations of the antenna inside-car and outside-car cases are also computed over multiple test runs. The results as a function of the antenna position (inside or outside the car) are compared for each test location and frequency. Finally, models for the path loss, which consist of the path loss exponents, attenuation intercepts, and standard deviations, are tabulated and compared for each location, antenna position, and frequency. Chapter 5 provides discussion and final remarks. References and Appendices follow the last chapter.

Chapter 2. Analytical Path Loss Formulas, and Antenna Patterns

2.1 Path Loss Calculation

Path loss is the measure of the attenuation a signal experiences as it propagates through a channel. Mathematically path loss ℓ is defined as the ratio p_t/p_r, where p_t is the transmitted power and p_r the received power. Typically this is represented in decibels (dB), as L (dB) $=10log(p_t/p_r)$. A channel is whatever medium or media the signal propagates through on its way from transmitter to receiver. In a wired or guided wave system this loss is (mostly) deterministic and well-studied, and the signal can propagate nearly exclusively through the guiding medium, typically composed of some conductor and some dielectric. However, wireless channels can be much more complex, and less controlled. For terrestrial communications, the signal will propagate through air typically, but it is often impossible to know exactly how it will behave in a given environment. In the most basic environment, the free space environment, there is nothing to impede the signal as it propagates from transmitter to receiver. This direct component that travels in a straight path from the transmitter to the receiver is known as the line-of-sight (LOS) component. Despite this the signal will still attenuate in this free-space environment as it propagates, and this attenuation is known as free-space path loss (FSPL), the equation for which is [6],

$$FSPL = \left(\frac{4\pi d}{\lambda}\right)^2 \tag{2.1}$$

where d is the distance between the transmitter and the receiver and λ is the wavelength of the signal. This model can most often be viewed as a minimum attenuation the signal will

experience as it propagates, although there are special cases of channels that can experience less than free-space attenuation. This FS model refers to an idealized environment that is not typically found on earth and is thus not realistic for terrestrial based communication systems. The two-ray path loss model is similar to the free-space model but includes an obstacle (generally approximated as a plane) from which the signal reflects. In many cases the obstacle is the earth. This reflected component then will either add constructively or destructively to the LOS component, depending on the phase relationship at the receiver. Figure 1 is a diagram of the 2-ray model.

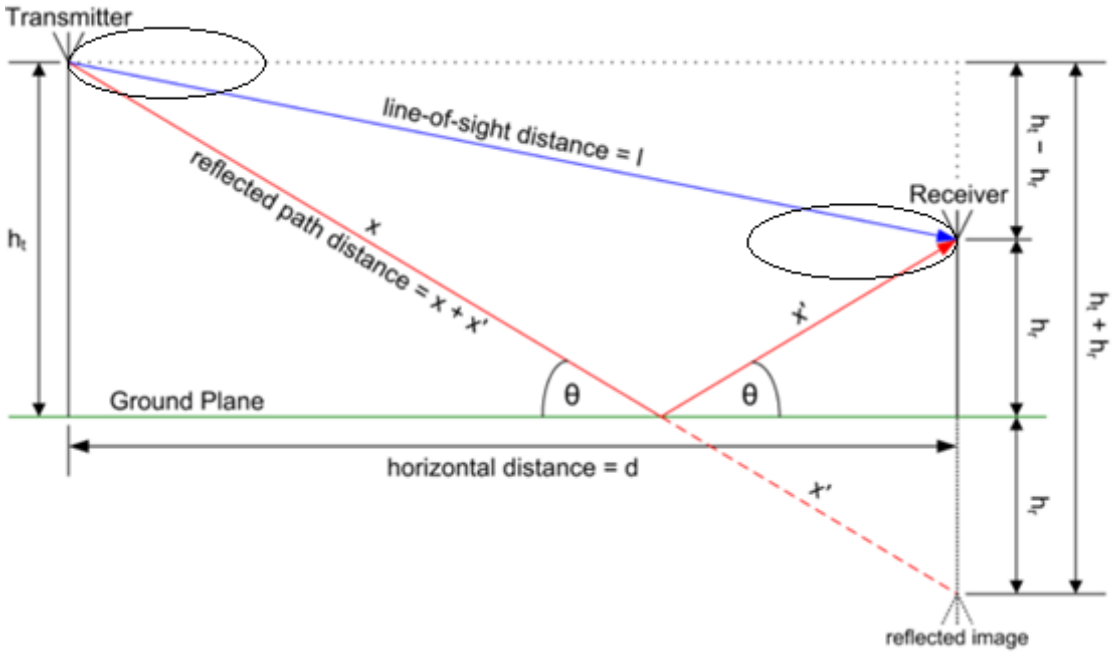

Figure 2.1. Diagram of the two-ray ground reflection model.

This model is dependent on the height of the antennas and the distance between them. These geometric parameters, along with the electrical properties of the ground plane from which the signal reflects, are used to calculate the reflection coefficient, which

determines the relative strength of the reflected signal. The two-ray path loss model is shown in (2.2) [6],

$$P_r = P_t \left(\frac{\lambda}{4\pi}\right)^2 \left|\frac{\sqrt{G_{los}}}{l} + \Gamma(\theta)\sqrt{G_{gr}}\frac{e^{-j\Delta\phi}}{x+x\prime}\right|^{-2} \tag{2.2}$$

where P_r is the received power, P_t is the transmitted power, G_{los} is the combined LOS gains of the transmit and receive antennas, G_{gr} is the combined ground reflection gains of the transmit and receive antennas, and $\Delta\phi$ is the phase difference between the paths given by (2.3):

$$\Delta\phi = \frac{2\pi\Delta d}{\lambda}. \tag{2.3}$$

The combined gains are the products of the Tx and Rx antennas gains for the given path (LOS and ground reflection paths). This is illustrated in Figure 2.1, where the ovals at the Tx and Rx represent each antenna's gain pattern. Where the blue LOS and the red reflected paths intersect these ovals represents the gains these individual components encounter as they propagate. When there is constructive interference between the two components, the attenuation of the signal can become less than that of free space. To find the path loss from these equations we create a link budget for the system (2.4),

$$PL = -P_r + P_t + G_t - L_t + G_r - L_r \tag{2.4}$$

where G_t is the transmitter gain, L_t is the cable loss at the transmitter, and G_r and L_r are the gain and cable loss of the receiver, all in dB. Thus, by using our measured received power we can predict the expected path loss of the channel.

2.2 Antenna Gain Patterns and Low Height Antennas

Antenna patterns or radiation patterns are a representation of how well the antenna radiates (and receives) power in a given direction. These patterns represent the three-dimensional power density of the antenna and are often represented as 2D "slices." An

example is shown in Figure 2.2a, of a pattern for an omni-directional antenna; the 3D diagram of the entire pattern appears in Figure 2.2b.

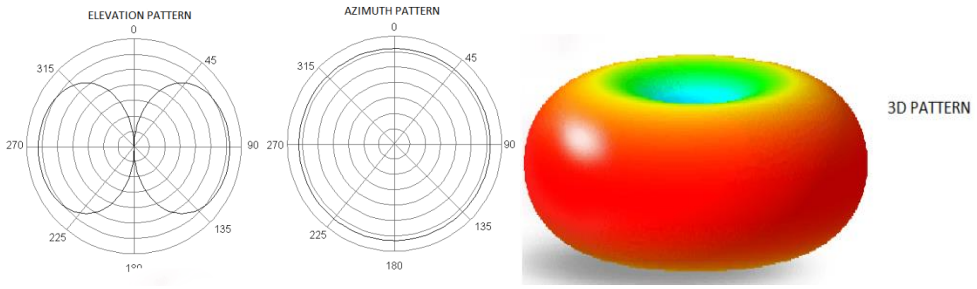

(a) (b)

Figure 2.2. Radiation pattern of an omnidirectional antenna (a) 2D cross sections, and (b) 3D model.

The omnidirectional antenna is named such because it radiates equally in all radial directions [9]. Radiation patterns generally assume that the antenna is radiating in a free space with no obstructions to block or change any part of the pattern. If this is not the case, the pattern can look drastically different because of the signal components reflected from or absorbed by the obstruction. For this reason, stationary antennas are typically mounted in a way to keep them away from obstacles, including the ground. This is not the case with the antennas used in this thesis: the transmitting antenna will be very close to the ground and this will have an effect on the radiation pattern. There are two types of antennas used in this thesis, monopole and log-periodic. These antennas have very different antenna patterns. The monopole has an omni-directional antenna pattern as seen in Figure 2.3.

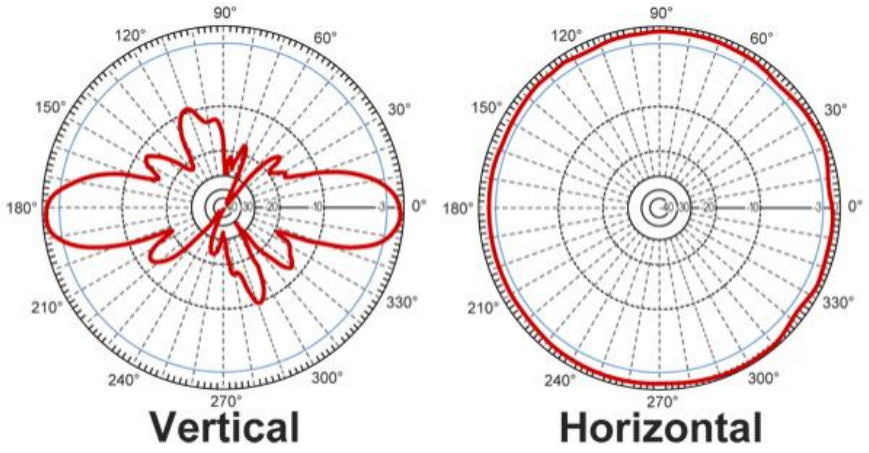

Figure 2.3. Antenna pattern of the L-Com Monopole antenna [10].

The log-periodic antenna has a more directional pattern. Its pattern has a beamwidth of approximately 90° as seen in Figure 2.4.

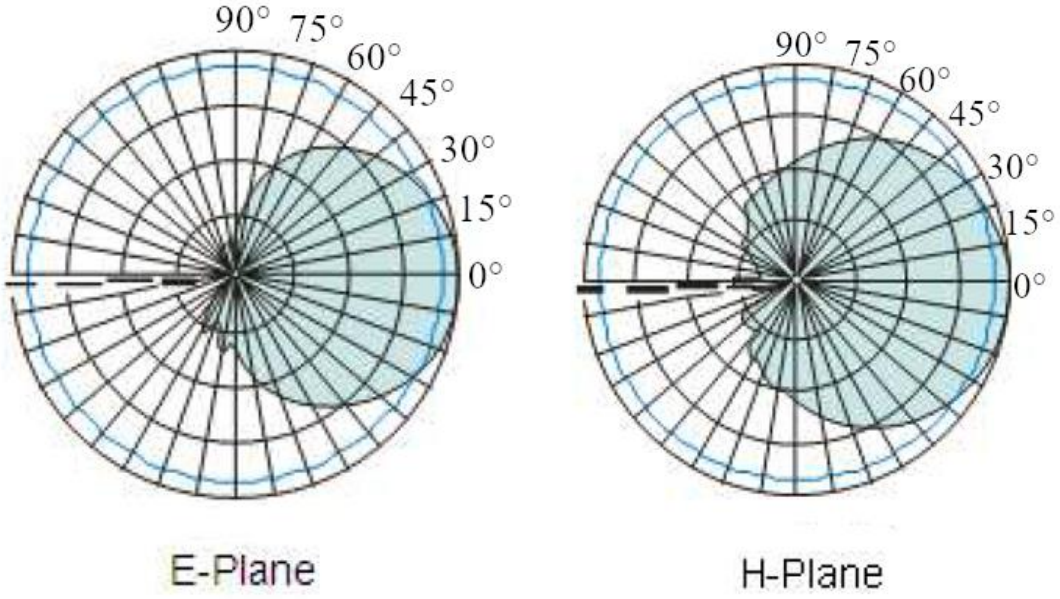

Figure 2.4. Antenna pattern of the RF Engineering Log-Periodic antenna [11].

We cannot know exactly how the pattern will be affected by the ground, but we can make some assumptions about how it will affect the transmission of the signal based on

what we know about the geometry and estimates of the ground electrical parameters. First, for the monopole antennas we know that a monopole positioned directly above a perfect ground plane will have the same pattern as a dipole positioned in free space [10]. The asphalt of the road is not a perfect ground plane in both composition and dimension, but this does give us a good approximation. For the log-periodic antenna we can assume that pattern will be more affected than the monopole pattern as the log-periodic antenna pattern has a wider 3 dB beamwidth in the elevation plane, meaning more of the signal will be directed towards the ground. The monopole antenna has a narrower beamwidth so more of the signal will be directed horizontally over the ground.

When a dipole antenna is placed above an infinite perfectly conducting ground plane the effect on the pattern is dependent on the height of the antenna above the plane. As seen in Figure 2.5, the number of minor lobes increases with antenna height. Neither of our antennas are dipoles but this does give us an indication of how the patterns will change. For the three frequency bands used in this work, 700 MHz, 2.4 GHz, and 5 GHz, the wavelengths are approximately 43, 12.5 and 6 cm respectively. Given that the antennas are positioned approximately 10 cm from the ground we can infer that the 2.4 and 5 GHz antenna patterns could be subject to additional lobes since the antenna height is near or even greater than a wavelength for these frequencies. The 700 MHz antenna pattern will be affected as well, but likely not nearly as much as the patterns for the higher frequencies, since the 700 MHz antenna is positioned about $\lambda/4$ distance above the ground [12].

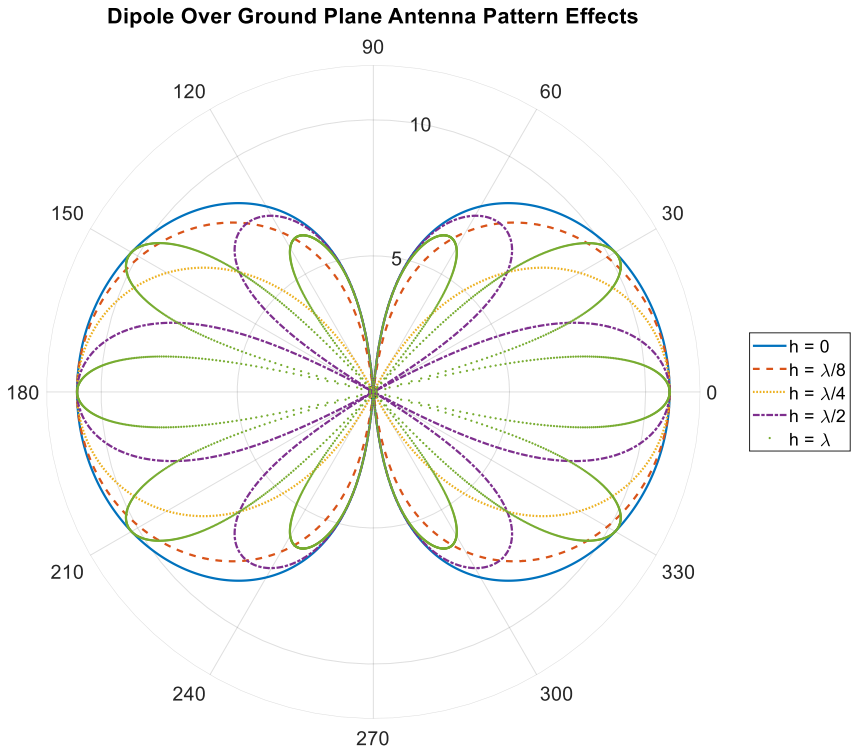

Figure 2.5. Effect of a ground plane on dipole antenna pattern for five different antenna heights.

For both antennas, the reflection of the signal from the asphalt of the road will be the most dominant component of the received signal after the LOS component. There may be other objects in the environment that can also cause scattering and multipath components to reach the receiver, but since for our measurements such objects were distant, we expect their strength will typically be less than that of the ground reflection. The equation for the vertically polarized reflection coefficient is given in (2.4) [6],

$$\Gamma_V = \frac{\left(\frac{\varepsilon}{\varepsilon_0} - j\sigma/\omega\varepsilon_0\right)\sin\theta - \sqrt{\left(\frac{\varepsilon}{\varepsilon_0} - j\sigma/\omega\varepsilon_0\right) - \cos\theta^2}}{\left(\frac{\varepsilon}{\varepsilon_0} - j\sigma/\omega\varepsilon_0\right)\sin\theta + \sqrt{\left(\frac{\varepsilon}{\varepsilon_0} - j\sigma/\omega\varepsilon_0\right) - \cos\theta^2}} \tag{2.4}$$

where ε is the relative permittivity of the medium the signal impinges on and ε_0 is vacuum permittivity, σ is the conductivity of the medium the signal impinges, ω is angular

frequency and θ is the angle with reference to the medium the signal impinges. The values for relative permittivity and conductivity of asphalt were 4.5 and 7.1 mS/m [13]. Since the transmitter is near the ground, when the receiver is far relative to the transmitter height, the angle of reflection, θ from Figure 2.1, is very small. When this happens, the sine terms in (3) become close to zero and the reflection coefficient can be approximated as -1. Thus, we can assume that the reflection coefficient varies slowly at longer distances but as the vehicle drives closer to the transmitter it will vary more rapidly. Near the transmitter we expect lower power reflections for both antennas. As the car drives closer to the transmitter it moves out of the "boresight" of the transmitting antenna. The boresight of an antenna is the direction of maximum gain of an antenna pattern, also called the peak of the main lobe. In the case of the log-periodic antennas, as the vehicle moves closer to the transmitter the antennas move further out of boresight as the angle of incidence increases. From Figure 2.4 we see that this means that the antenna gains decrease with distance.

Chapter 3. Test Procedures

3.1 Test Locations

The tests were performed in two locations in Columbia, South Carolina. The first was on Main St. outside the engineering building Swearingen Engineering Center. This location is urban as there are buildings flanking the street and the road itself is four lanes, seen in Figures 3.1 and 3.2.

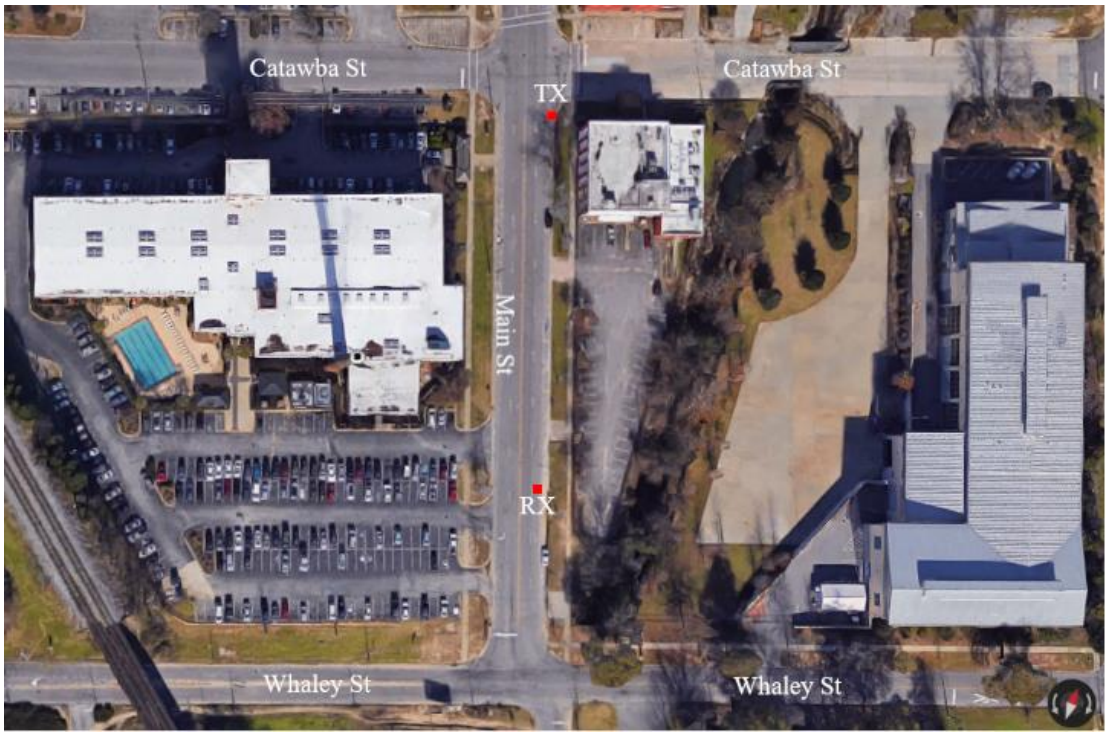

Figure 3.1. Main St. test location, satellite view, from Google Maps ®.

Figure 3 2. Main St. test location street view, looking approximately south.

The second location, Simmon Tree Lane, is more rural: it is a two-lane road with no nearby buildings or trees, and only fields on both sides of the road, seen in Figures 3.3 and 3.4. This location was specifically chosen to act as a reference case. Since the environment is open fields, there will be fewer multipath components than in the Main St. location.

Figure 3.3. Simmon Tree Lane test location, satellite view, from Google Maps ®.

Figure 3.4. Simmon Tree Lane location street view.

Figure 3.5 shows a diagram of the path the receiver (RX) vehicle followed at each test location. For each location and each trial, the RX began 100 m away from the transmitter (TX) and drove in a straight path toward the TX. Once the vehicle reached the transmitter, the power recording stopped and the car returned to the start location for another trial.

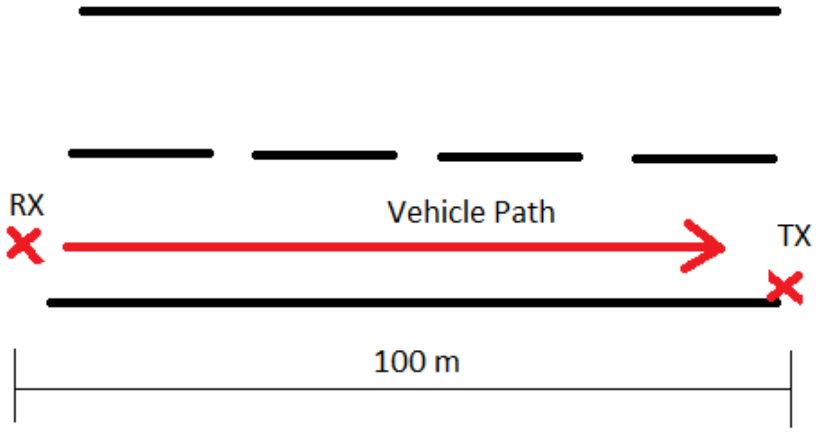

Figure 3.5. Path traveled by Rx in reference to the Tx.

3.2 Test Equipment

3.2.1 Transmitter Equipment

The full list of test equipment is provided in Table 3.1.

Table 3.1. Test Equipment list.

Name	Manufacturer	Model Number
Signal Generator	Keysight	N5182A MXG
Spectrum Analyzer	Keysight	N9342C
Log-periodic Antennas	RF Engineering	RFCA-727-11
Monopole Antennas	L-Com	HGV-4958-06U
Coax Cables (N-type)	Pasternack	LMR-195
Power Inverter	OSP	1500W-PSW
Car Battery	Duracell	SLI3MDC

The transmitter system consists of the signal generator, transmitting antenna, power inverter, cables and connectors, and a marine battery. Since the test took place along roadsides, outlets to power the equipment were unavailable. To provide portable power a marine battery and power inverter were used. The car battery supplied a 12 V DC signal, and the power inverter converts this to 120 V AC, the same as a typical US wall outlet. The power inverter has two outlets, only one of which the signal generator uses. This setup can power the signal generator for well over an hour with a fully charged battery; a second battery was present if needed. The signal generator, power inverter, and car battery are shown connected in Figure 3.6.

Figure 3.6. Signal generator, power inverter and car battery.

The transmitting antenna depends on the frequency of the test. For the 700 MHz and 2.4 GHz band tests, our log periodic antennas were used. One of these is shown in Figure 3.7, attached to a tripod. For the 5 GHz band tests, the antennas used were the monopoles shown in Figure 3.8.

Figure 3.7. Log-periodic antenna mounted on tripod.

Figure 3.8. Monopole antenna mounted on box.

The transmitting antenna was connected to the signal generator via N-type coax cable. Since the goal of these tests is to measure attenuation as a function of distance for a near-ground antenna to vehicle channel, the transmitting antenna must be placed as near to the ground as possible. The log-periodic antenna was taped to a small flat board to keep it steady during testing; see Figure 3.9. The monopoles were mounted to cardboard boxes to keep them stable during testing, as seen in Figure 3.8.

The transmitting antenna must be aimed at the receiver during the test because the log-periodic antennas are directional. In the case of the monopole antennas the direction they face is not important so long as they remain vertical, since they are omni-directional. The log-periodic antennas however, have approximately a 90° beamwidth and must be aimed down the road toward the vehicle.

Figure 3.9. Transmitting antenna (log-periodic) on the ground aimed at the receiver in the car 100 m away.

3.2.2 Receiver Equipment

The receiver consisted of the Keysight N9342C portable spectrum analyzer, and the receiving antenna, with an N-type coax cable to connect them. The spectrum analyzer is powered by its own rechargeable battery. The receiver is set within the test vehicle and the antenna is positioned in the passenger seat for one set of tests and on the roof of the vehicle for the other set. These two antenna positions can be seen in Figure 3.10.

(a) (b)

Figure 3.10. Receiving antenna and spectrum analyzer. (a) Antenna in car, and (b) Antenna secured to roof of car using painter's tape.

3.3 Test Procedure

To start, the receiver vehicle was positioned 100 m down the road from the transmitter. When the team member who was operating the spectrum analyzer and the driver were ready, they signaled to the team member at the transmitter that they may begin transmitting. The signal generator was then set to output a constant single tone signal, the equation for which is (2.1), where ω_c is equal to $2\pi f_c$, and f_c is the center frequency and A is the amplitude of the signal, 50 mV,

$$s(t) = A\cos(\omega_c t) \tag{3.1}$$

Once the signal generator began transmitting, the driver slowly (about 5 mph) drove toward the transmitter. The spectrum analyzer recorded the received power as the car moved along its path. The spectrum analyzer measured the peak of the received signal. The starting distance of 100 m was chosen arbitrarily but the goal was to measure the attenuation of the channel over a moderate link distance for which vehicular applications are planned. Once the vehicle reached the transmitter, the recording was stopped, and the car returned to the start location for another trial or "pass." Four trials were done at each frequency and antenna placement resulting in twenty-four trials, tabulated in Table 3.2.

Table 3.2. Trial Types Used for Testing

Trial	Antenna Position	Frequency (MHz)
1	Inside Car	700
2		
3		
4		
5		2400
6		
7		
8		
9		5000
10		
11		

12		
13	Outside Car	700
14		
15		
16		
17		2400
18		
19		
20		
21		5000
22		
23		
24		

Chapter 4. Results

4.1 Attenuation vs. Distance

The primary result we consider is attenuation, or path loss, versus distance. In this experiment there were two locations, and for each location, two antenna positions and three frequencies, with four trials per location, frequency and position, totaling forty-eight trials listed in Table 3.2. We plot the measured attenuation versus distance, as well as the freespace path loss and the two-ray model path loss versus distance for comparison.

4.1.1 South Beltline Location, Antenna Outside Car

The first set of results presented is for the trials at the Beltline location with the antenna outside the vehicle, in Figures 4.1-4.4. Figure 4.1 shows results for each of the four trials for the 700 MHz case separately. The first thing to note is how similar the measured path loss is for each of the four trials, as we might expect. Each trial has nearly the same slope and intercept as the attenuation increases with distance. The plots all have intercept 49 dB at distance equal to 3.5 m and attenuation increases to approximately 98 dB at distance 100 m from the transmitter. In the following figures for this subsection the attenuation versus distance of each of the four trials for each frequency and location are shown overlain. The average attenuation over all four trials is also shown, along with the linear fit to this average, and the freespace and 2-ray path loss models.

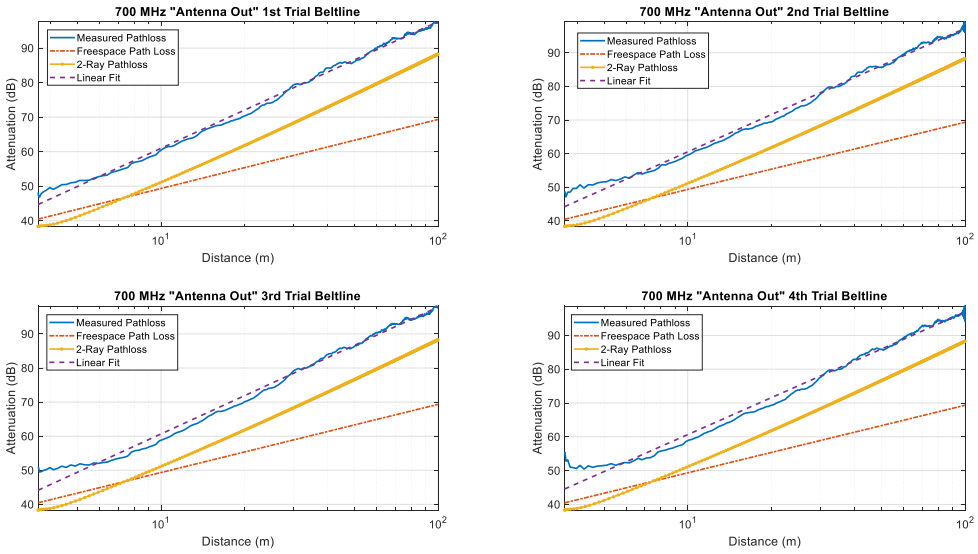

Figure 4.1. 700 MHz, Antenna Outside Vehicle, South Beltline, path loss vs. distance results for all four trials separately, including freespace and two-ray path loss, as well as the linear fit line to the measured data.

The similarities in the results of the trials can more clearly be seen in Figure 4.2 where the attenuation results from each of the trials are overlain in a single plot. Each trial's attenuation is on average about 9 dB larger than the 2-ray path loss.

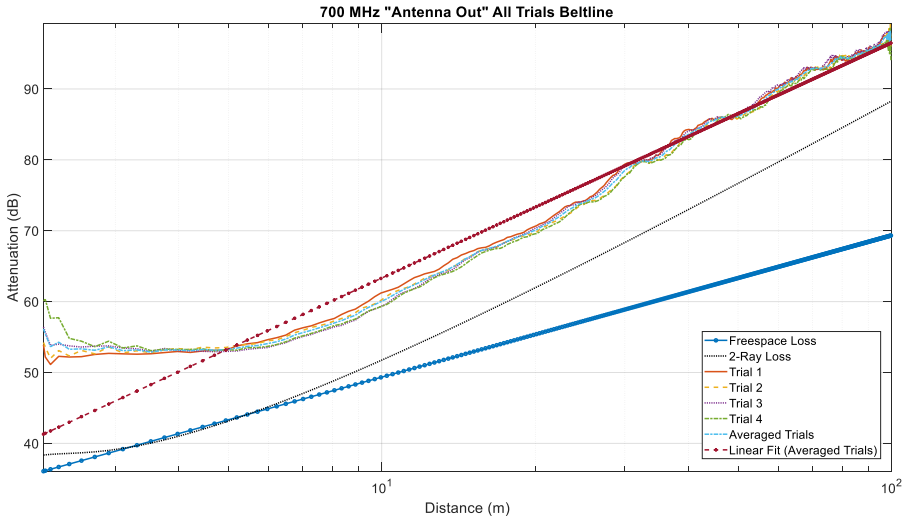

Figure 4.2. 700 MHz, Antenna Outside Vehicle, Beltline, path loss vs. distance for all four trials along with freespace, two-ray, the averaged trials attenuation and a linear fit to the measured data.

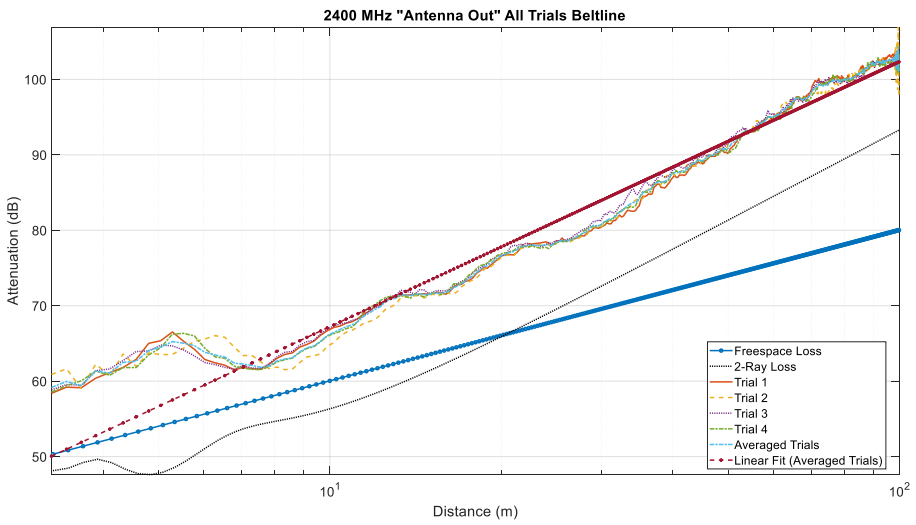

Figure 4.3. 2400 MHz, Antenna Outside Vehicle, Beltline, path loss vs. distance for all four trials along with freespace, two-ray, the averaged trials attenuation, and a linear fit to the measured data.

Just like the 700 MHz trial results, the 2.4 GHz trials all show similar structure versus distance; see Figure 4.3. The measured results' linear fit attenuation is approximately 11 dB larger than that of the two-ray model attenuation. The 5 GHz results in Fig. 4.4 are similar to one another over the distance range but there is greater variation among the trials than at the other frequencies, especially for short distances (when the Rx is near the transmitter). The attenuation of the trials oscillates rapidly until about 11 m, and this is attributable to multipath components (MPCs). As the distance increases there is less variation among the trials and the attenuation of each trial increases to approximately 98 dB at 100 m; this behavior is analogous to that of the theoretical two ray model. The 5 GHz trials' attenuation is greater than the 2-ray path loss over the entire test interval. The attenuation varies from 7 to 30 dB greater than 2-ray near the transmitter before decreasing to 5 dB near 100 m, where the 30 dB value pertains to the MPC attenuation peak.

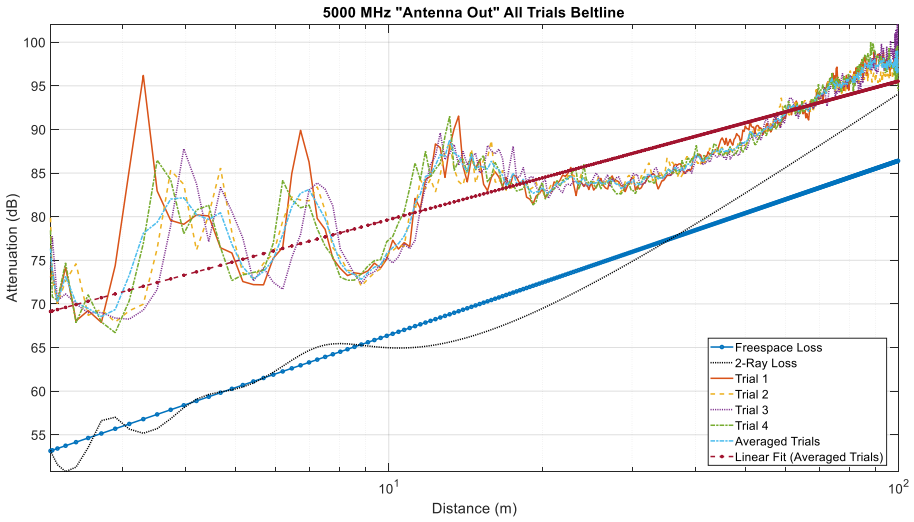

Figure 4.4. 5000 MHz, Antenna Outside Vehicle, Beltline, path loss vs. distance for all four trials along with freespace, two-ray, the averaged trials attenuation, and a linear fit to the measured data.

4.1.2 South Beltline Location, Antenna Inside Car

For this set of trials, the antenna is positioned inside the vehicle. This means that the signal must now propagate through the car to be received by the antenna. In addition, the antenna heights are naturally different: approximately 2 m outside the car, and 1.1 m inside the car. We expect a larger attenuation than the outside antenna case. These effects are depicted in Figures 4.5-4.7. Similar to the other cases, the results of the 700 MHz trials with the antenna inside the vehicle follow the same general pattern. The attenuation of the trials is generally larger than that of the 700 MHz trials in Figure 4.2, as noted. For example, at d=10 m, the inside-car case attenuation is 10 dB larger than that for the antenna outside the vehicle trials. There is also an attenuation peak seen in each of the trials at 77 m where the attenuation reaches about 106 dB.

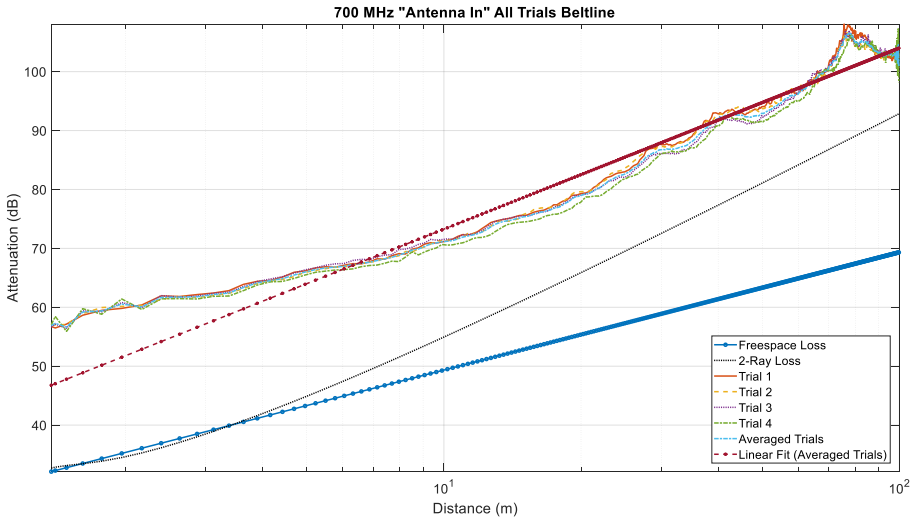

Figure 4.5. 700 MHz, Antenna Inside Vehicle, Beltline, path loss vs. distance for all four trials along with freespace, two-ray, the averaged trial attenuation, and a linear fit.

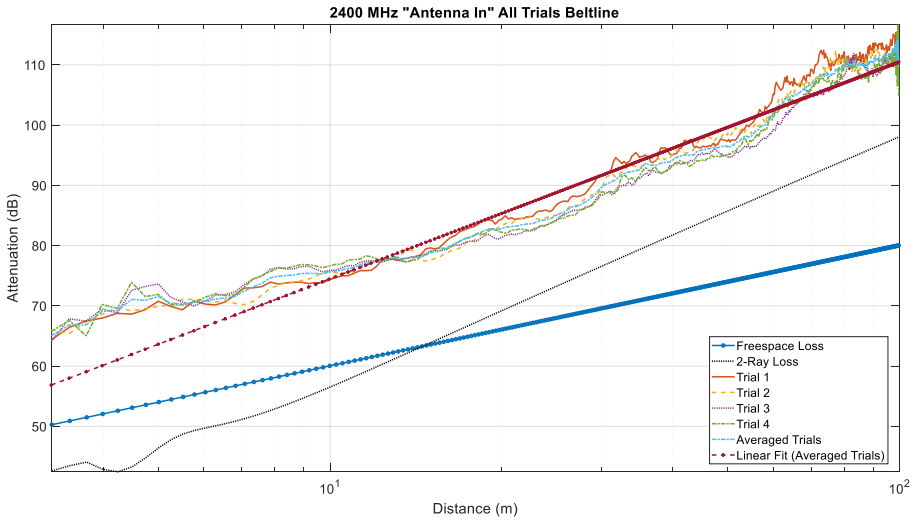

Figure 4.6. 2400 MHz, Antenna Inside Vehicle, Beltline, path loss vs. distance for all four trials along with freespace, two-ray, the averaged trials attenuation, and a linear fit.

Figure 4.6 displays more small-scale fading compared to the inside-car attenuation in Figure 4.3. This is due to multipath reflection, scattering, and diffraction associated with

the signal traveling from outside to within the vehicle. The attenuation is about 10 dB larger than the antenna outside car trials over the entire distance interval.

Figure 4.7 shows the attenuation of the trials varies more significantly at the 5 GHz frequency. This is again due to small scale fading from the antenna position inside the car. As with the 2.4 GHz trials, the 5 GHz trials have approximately 10 dB larger attenuation than the results where the antenna is outside the vehicle. We discuss the differences between inside and outside-car antenna cases subsequently; Table 4.1 shows the difference in attenuation between the inside-car and outside-car cases for each frequency and location.

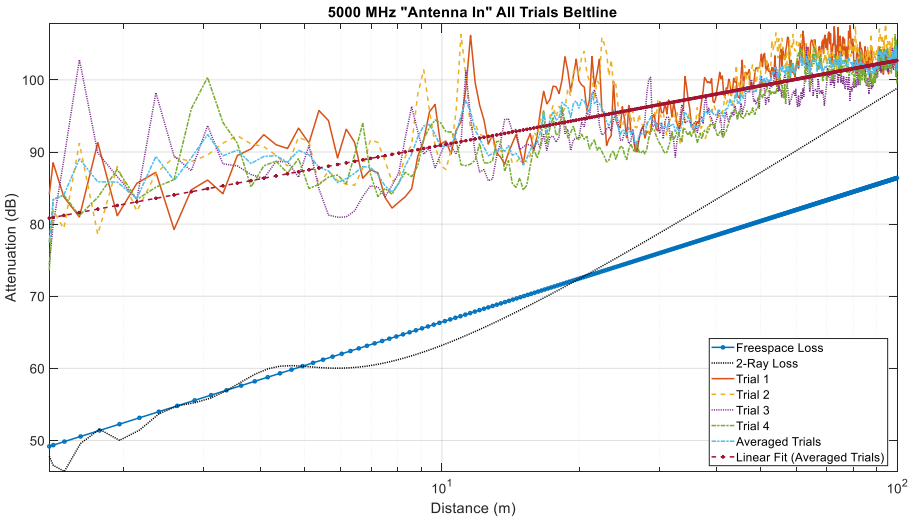

Figure 4.7. 5000 MHz, Antenna Inside Vehicle, South Beltline, path loss vs. distance for all four trials along with freespace, two-ray path loss, the averaged trials attenuation, and a linear fit.

4.1.3 Main St. Location, Antenna Outside Car

Figures 4.8-4.10 show the results for the trials for a different location, Main Street. The Main Street location is different from the South Beltline location in that it is a more urban setting. There are buildings on both sides of the street and more objects along the street, such as parked cars, fences, bushes, street lamps, etc. The attenuation of the trials in the Main Street location is more variable than in the Beltline trials. This is due to the larger

number of multipath components being received. In the Beltline trials the test area is flat and thus there are not many opportunities for the signal to reflect from an object and be directed to the Rx. It is also worth noting there is smaller difference between the attenuation of the average trial attenuation and the 2-ray model attenuation than in the Beltline cases.

Figure 4.8 shows close agreement between the results of the four trials with attenuation peaks occurring at roughly the same intervals in each trial. The attenuation is approximately the same as the 700 MHz, antenna outside the vehicle trials for the Beltline location. The difference between the Beltline and Main St locations can be expressed in terms of the path loss exponent *n* and the standard deviation σ of the log-distance linear fit models. The path loss exponents are 2.97 and 3.32 for the Main St. and Beltline locations, respectively, for the 700 MHz, antenna outside-car cases. The standard deviations are 11.02 and 13.08 for the same cases.

Similar observations pertain to how the antenna position affects these parameters. The inside the vehicle antenna position trials typically have lower path loss exponents and standard deviation than the outside the vehicle trials. The intercept point remains typically the same in each location and antenna position but increases with frequency, as expected.

Figure 4.9 shows agreement for 2400 MHz between the results of the four trials over the test interval. Also worth noting is the quasi-periodic nature of the attenuation peaks appearing at the larger distances. This is typically a characteristic of the two-ray model at short distances, but here we incur some strong multipath effect particular to the geometry of this trial location.

Figure 4.10 is similar to the figures showing results for other 5 GHz trials, in that over most of the test interval the trial attenuation does not agree very closely with the

models. This is not surprising since the two models are quite simple and cannot account for the multiple propagation mechanisms (reflection, scattering, and diffraction) in effect in this complicated environment.

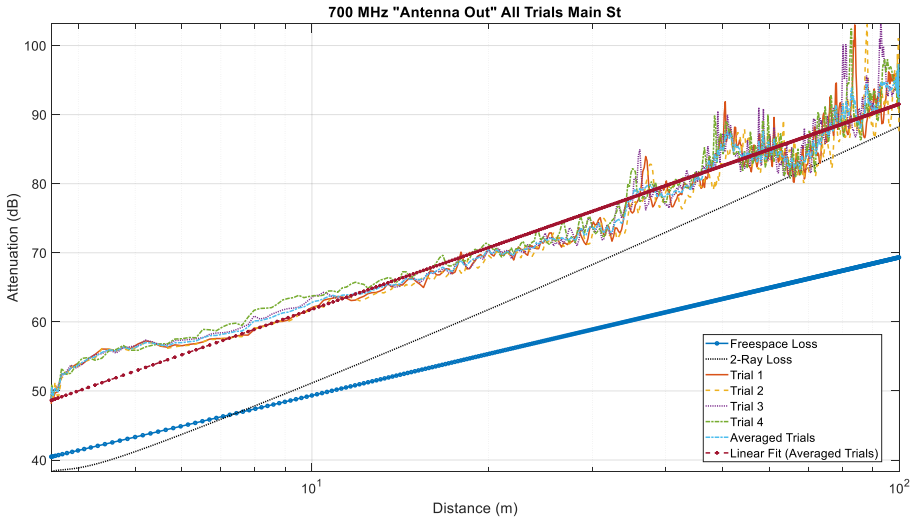

Figure 4.8. 700 MHz, Antenna Outside Vehicle, Main St, path loss vs. distance for all four trials along with freespace, two-ray path loss, the averaged trials attenuation, and a linear fit.

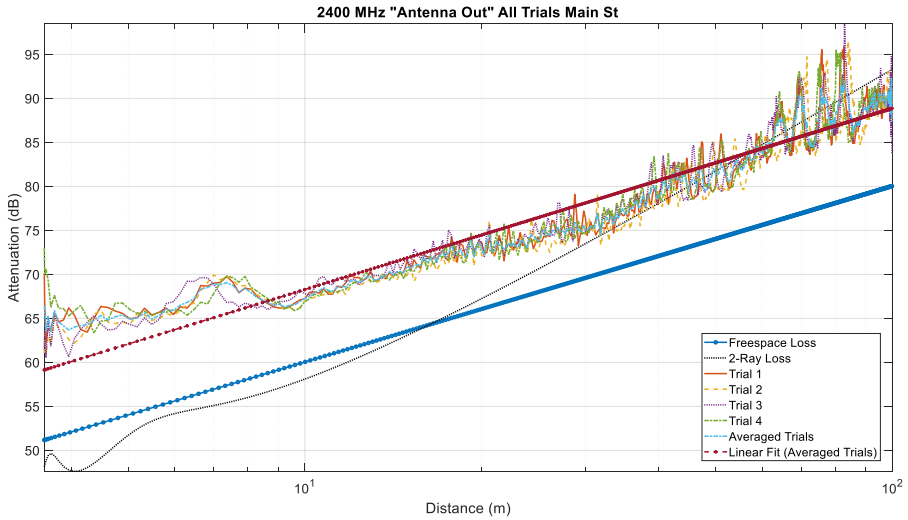

Figure 4.9. 2400 MHz, Antenna Outside Vehicle, Main St, path loss vs. distance for all four trials along with freespace, two-ray path loss, the averaged trials attenuation, and a linear fit.

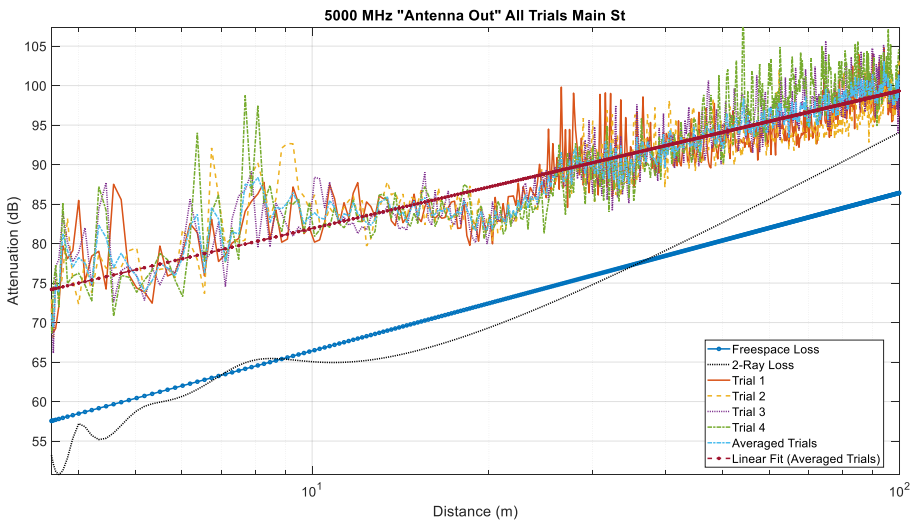

Figure 4.10. 5000 MHz, Antenna Outside Vehicle, Main St, path loss vs. distance for all four trials along with freespace, two-ray path loss, the averaged trials attenuation, and a linear fit.

4.1.4 Main St. Location, Antenna Inside Car

The final subsection of this section shows the results of the trials for the Main St. location where the antenna is again outside and on top of the car in Figures 4.11-13. In Figure 4.11 the attenuation of the inside-car trials is again larger than that of the antenna outside-car trials of the Main St. location, similar to the Beltline antenna inside-car trials. The main difference is the attenuation peaks are larger than in the antenna outside-car case, most likely due to additional MPCs from within the vehicle. Figure 4.12 shows that for the 2400 MHz frequency, we have larger measured attenuation than in the antenna outside the car results for the same frequency and location (about 5 dB larger), with even more pronounced quasi-periodicity at distances greater than 40 m. This quasi-periodicity is also a function of the measurement geometry for this location, where at these larger distances, multipath component interference is significant.

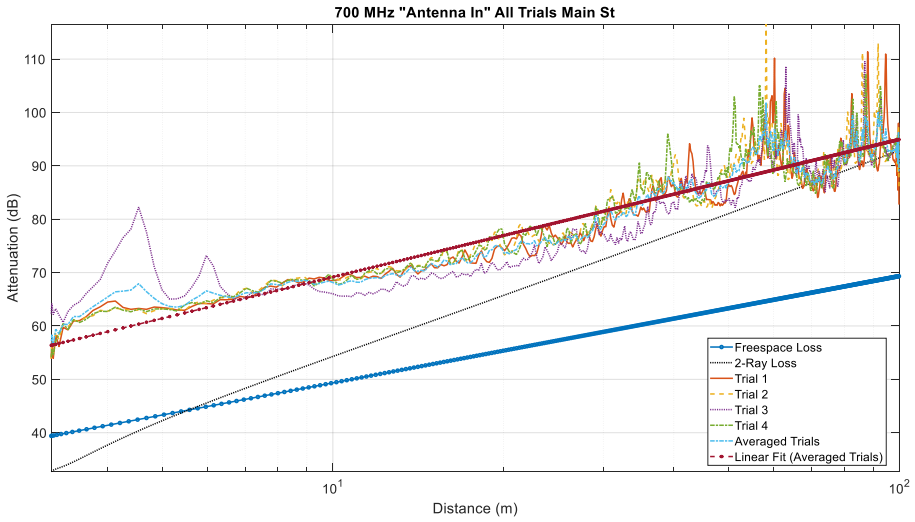

Figure 4.11. 700 MHz, Antenna Inside Vehicle, Main St, path loss vs. distance for all four trials along with freespace, two-ray path loss, the averaged trials attenuation, and a linear fit.

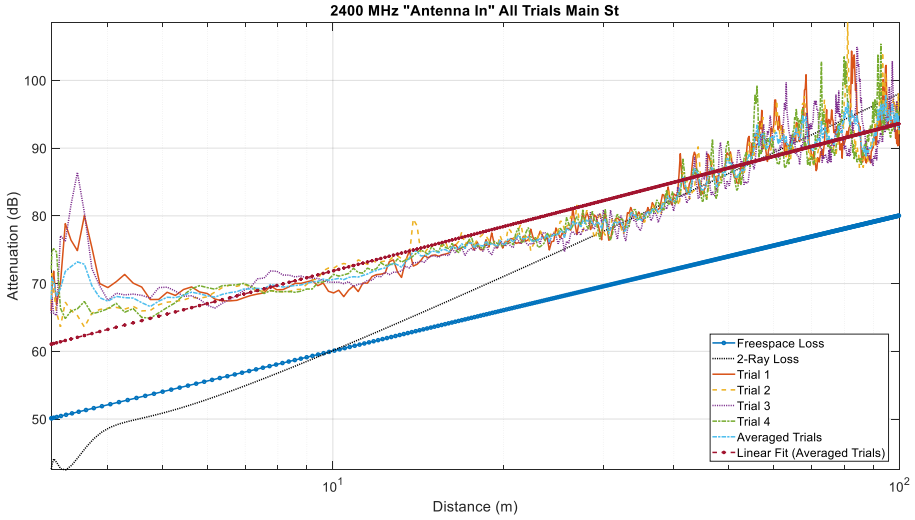

Figure 4.12. 2400 MHz, Antenna Inside Vehicle, Main St., path loss vs. distance for all four trials along with freespace, two-ray path loss, the averaged trials attenuation, and a linear fit.

From Figure 4.13 it is clear that for the 5 GHz frequency, inside-car case, the trial results agree reasonably well with the 2-ray model beyond approximately 40 m. The measured attenuation is larger than the two ray values at smaller distances.

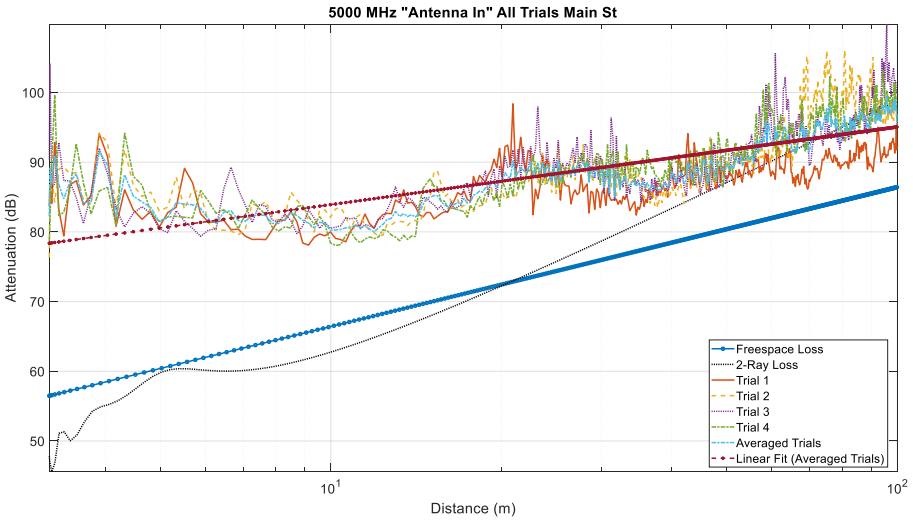

Figure 4.13. 5000 MHz, Antenna Inside Vehicle, Main St, path loss vs. distance for all four trials along with freespace, two-ray path loss, the averaged trials attenuation, and a linear fit.

Table 4.1 shows the difference between the linear fit of the average of the four trial's attenuation and the 2-ray path loss model attenuation. The smaller the differences (for both the maximum difference and minimum difference), the closer the linear fit model is to the 2-ray.

Table 4.1. Maximum, Minimum and average Difference Between Linear Fit and 2-Ray Attenuation.

Location	Antenna Position	Frequency (MHz)	Average Difference (dB)	Min Difference (dB)	Max Difference (dB)
Beltline	Antenna Outside Vehicle	700	9.7	2.9	11.6
		2400	10.2	1.9	12
		5000	8.6	1.5	18.8
		700	14.2	11.1	19.1

	Antenna Inside Vehicle	2400	14.3	12.4	18.7
		5000	14.1	3.9	35.5
Main St.	Antenna Outside Vehicle	700	6.5	3.2	11.7
		2400	2	0	12.7
		5000	12	5.3	23.7
	Antenna Inside Vehicle	700	7.6	2.1	23.7
		2400	2.4	0	19.1
		5000	6.8	0	32.8

From the table it is clear to see the Main St. location has a closer fit to the 2-ray model. Every value is much smaller than for the Beltline location except the max difference. The antenna outside the vehicle cases have closer fits to the 2-ray model than the antenna inside cases for both locations. Finally, the 2.4 GHz Main St. locations have the smallest average difference of about 2 dB and even intersect the 2-ray fit line in these cases.

4.2 Vehicle Effects

In this section the effects of the antenna position on path loss are compared. The attenuations of each of the four trials for each case were averaged and the average attenuation for each location and frequency is shown versus distance for both the antenna inside-car and outside-car cases. Figures 4.14-4.19 show these results for each location and frequency. As expected from the discussion in section 2.3, the attenuation at 700 MHz is larger when the antenna is inside the vehicle by approximately 7 dB for distances larger than 20 m. The 700 MHz Beltline trial results, seen in Figure 4.14, tend to follow a similar

pattern where the difference between the inside-car and outside-car trials has an attenuation peak at approximately 87 m. The antenna inside-car and outside-car cases have similar path loss exponents 3.07 and 3.32, respectively. This means the slopes of the fit lines are similar over the test interval. The biggest difference is the intercepts, the inside-car case is about 11 dB higher than the outside-car case at 59.74 dB versus 48.29 dB.

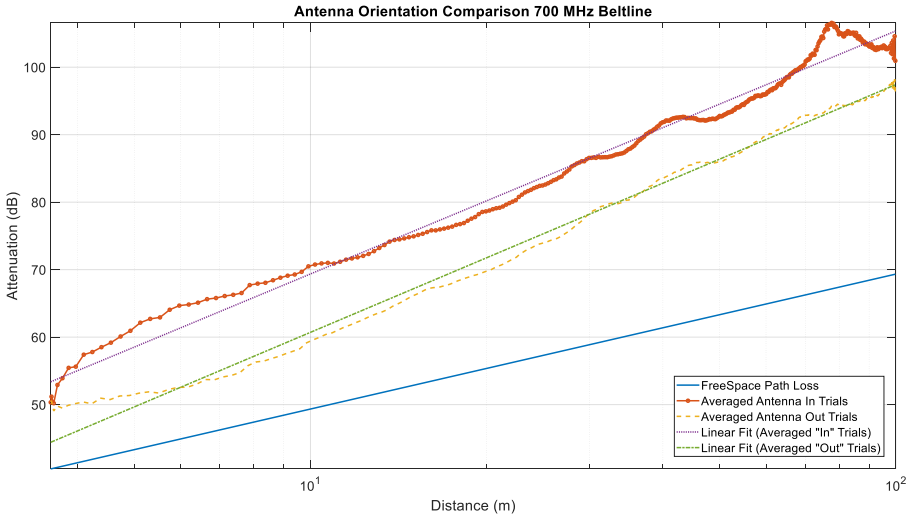

Figure 4.14. 700 MHz, Beltline location, path loss vs. distance antenna position comparison.

Similar to the 700 MHz trials, the antenna inside-car trials for the 2.4 GHz case, seen in Figure 4.15, have larger attenuation than the outside-car trials by approximately 5 dB for distances greater than 15 m. The difference between path loss exponents is even smaller for the 2.4 GHz Beltline cases than the 700 MHz cases, at 3.6 and 3.51 for the inside-car and outside-car cases, respectively. The difference between intercepts is also slightly smaller for the 2.4 GHz cases than the 700 MHz cases at approximately 7 dB. The inside-car intercept is 59.1 dB versus the outside-car intercept of 51.9 dB.

Just like the 700 MHz and 2.4 GHz trials for the Beltline location, the antenna inside-car trial results have a larger attenuation at 5 GHz over the entire range of distances.

The path loss exponents, for each 5 GHz case, are much lower than for the other frequencies. The exponents are 1.17 and 1.59 for the inside-car and outside-car cases, respectively. These cases also have the largest difference in intercepts, at approximately 13 dB, from 72.5 dB and 85.7 dB for the outside-car and inside-car, respectively. Notably, the oscillation of the attenuation at small distances seen in the antenna outside-car trials is not repeated in the antenna inside-car trials. This is likely attributable to the blockage of the ground reflection component by the car.

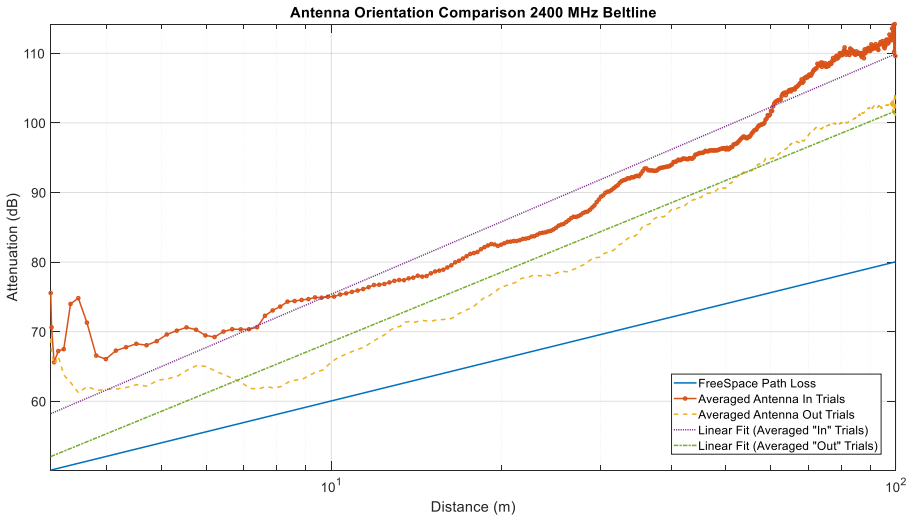

Figure 4.15. 2.4 GHz, Beltline location, path loss vs. distance antenna position comparison.

The 700 MHz trial results for the Main St. location show less of an attenuation difference between inside and outside antennas than observed in the Beltline trial results. The difference ranges from 3 to 6 dB between the inside and outside-car trials over the 10 – 50 m range. At distances greater than 50 m, the attenuation develops peaks for both cases, but of course the antenna inside-car results have larger peaks than the antenna outside-car trial results. The path loss exponents for this case are smaller than the exponents of the 700

MHz Beltline cases. They are 2.58 and 2.97 for the inside-car and outside-car cases, respectively, and the intercepts are 48.6 dB and 57.7 dB, respectively.

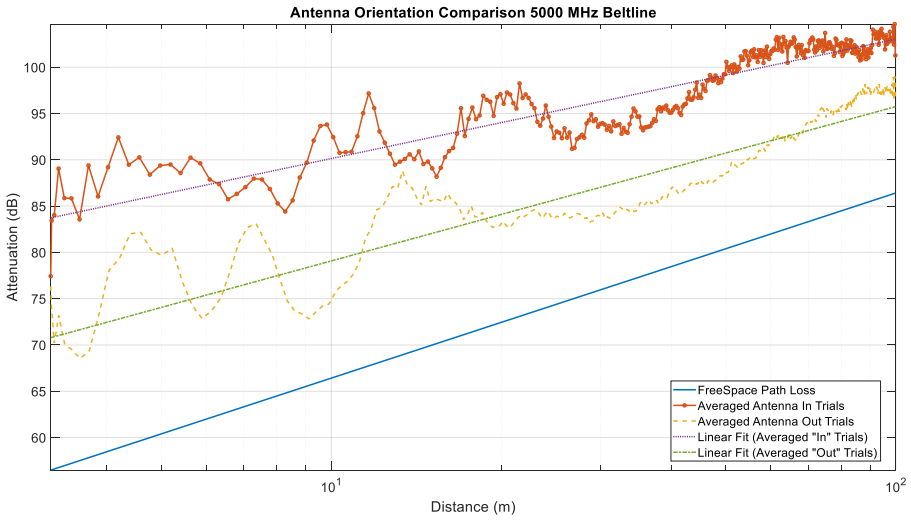

Figure 4.16. 5 GHz, Beltline location, path loss vs. distance antenna position comparison.

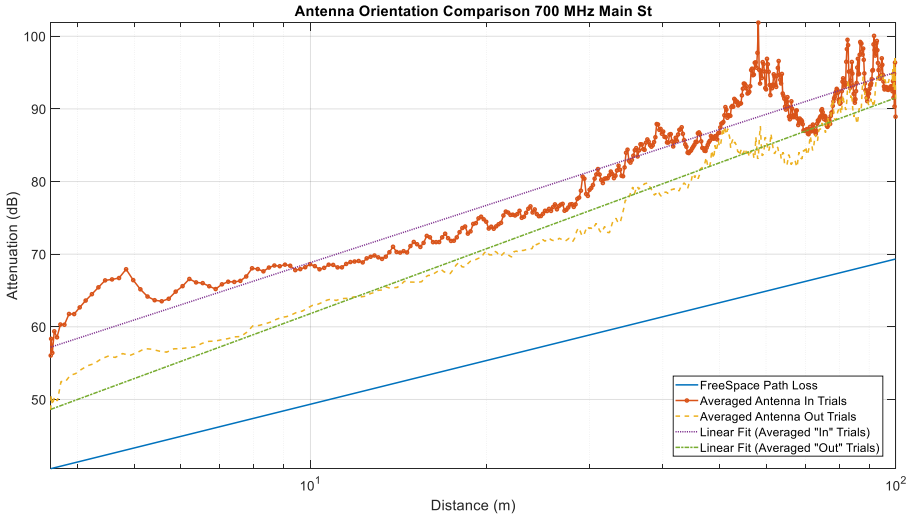

Figure 4.17. 700 MHz, Main St. location, path loss vs. distance antenna position comparison.

Similar to the 700 MHz case, the 2.4 GHz trial results have a very small difference in attenuation over the 10–50 m range. The quasi-periodicity begins after the 50 m distance

but the peaks are not as sharp for this frequency as for the 700 MHz case. The path loss exponents for these trials are much smaller than the Beltline trials, 2.06 and 2.17 for the outside-car and inside-car cases, respectively, compared to the 3.51 and 3.6 of the Beltline 2.4 GHz cases. This is again attributable to the waveguiding effect of the buildings along the street. The intercepts are the closest of any pair, approximately 3 dB apart, with value 59.1 dB for the outside-car case and 62.3 dB for the inside-car case.

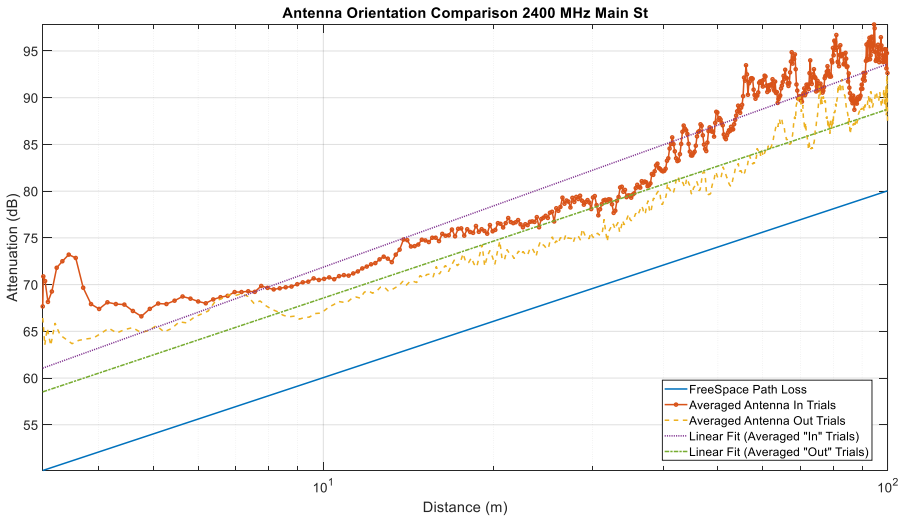

Figure 4.18. 2.4 GHz, Main St. location, path loss vs. distance antenna position comparison.

The 5 GHz trial results for the Main St. location are somewhat surprising: the attenuation of the antenna inside-car trials is *not* always larger than that for the outside-car trials. The outside-car attenuation becomes larger than the antenna inside-car trials at about 6 – 15 m and then again at distances greater than 25 m. This could be due to the fact that the 5 GHz antennas are omni-directional. The path loss exponent of the inside-car case is the lowest of all the cases at 1.11, and the exponent of the outside-car case is 1.74. This is again lower than the exponent of 700 MHz and 2.4 GHz frequency cases. Due to the difference in exponents and close values of intercepts (74.19 dB and 78.9 dB for the

outside-car and inside-car cases, respectively), the fit lines cross at the 20 m distance; this is the only set of cases to do so.

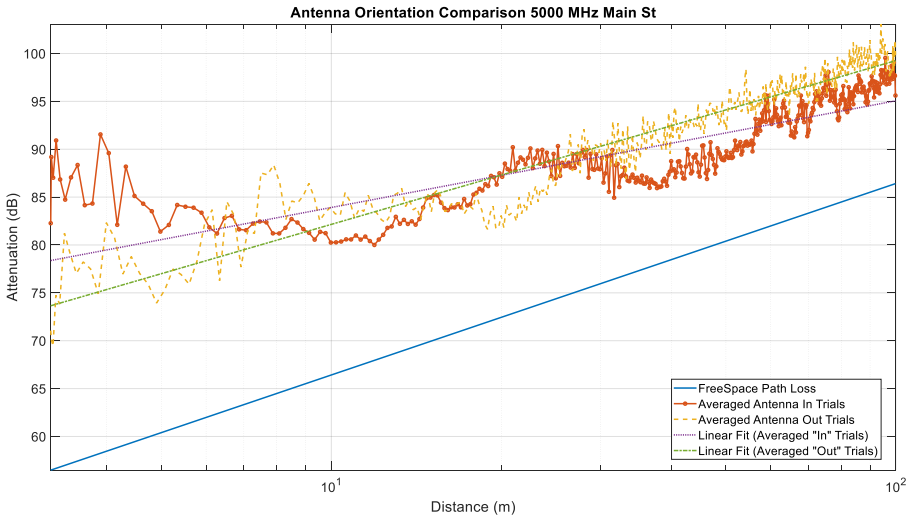

Figure 4.19. 5 GHz, Main St. location, path loss vs. distance antenna position comparison.

The 5 GHz Main St. minimum difference between the inside-car and outside car fit lines is 0 dB because as seen in Figure 4.19, this is the only case were the fit lines intersect one another. The largest maximum difference is found with the 5 GHz Beltline case with a difference of 12.9 dB. This is most likely due to the sparsity of MPCs in the Beltline environment, hence reducing the total received power. In fact the Main St. maximum and minimum differences are all lower than the values for the Beltline location at the same frequencies.

Table 4.1. Maximum and Minimum Difference Between Antenna Inside-car and Outside-car Fit Lines.

Location	Frequency	Average Difference (dB)	Min Difference (dB)	Max Difference (dB)	Standard Deviation (dB)

Beltline	700	8.2	8	9	0.3
	2400	7.6	6.1	8.2	0.5
	5000	8.9	7.3	12.9	1.4
Main St.	700	5	3.5	8.6	1.3
	2400	4.2	2.5	4.8	0.7
	5000	2.5	0	4.7	1.3

4.3 Path Loss Models

Table 4.3 shows the path loss exponent *n* and the standard deviation σ in dB for the results for the measured data averaged over all trials in each case. The path loss exponent quantifies the rate of increase in attenuation versus distance. A value of *n*=2 represents freespace path loss so any value less than 2 implies the signal propagates through the environment with lower than freespace attenuation, typically via MPCs. Conversely any value greater than 2 implies greater than freespace attenuation as the signal propagates through its environment.

Table 4. 2. Path Loss Exponent, Intercept, and Standard Deviation of the Averaged Trials for each Case

Location	Antenna Position	Frequency (MHz)	Path Loss Exponent *n*	Intercept 3.6 m (dB)	Standard Deviation σ (dB)
Beltline	Antenna Outside Vehicle	700	3.3	48.3	13.1
		2400	3.5	51.9	12.2
		5000	1.6	72.5	6.7
		700	3	59.7	12.7

	Antenna Inside Vehicle	2400	3.6	59.1	12.5
		5000	1.2	85.7	5.2
Main St	Antenna Outside Vehicle	700	3	48.7	11
		2400	2.1	59.1	7.8
		5000	1.7	74.2	6.6
	Antenna Inside Vehicle	700	2.6	57.7	10
		2400	2.2	62.3	8.5
		5000	1.1	78.9	4.9

Table 4.3 shows clear patterns in how the path loss exponent, intercept and standard deviation behave in the test environments. For the Beltline outside-car case, the exponent increases as the frequency increases from 700 MHz to 2.4 GHz. However, at 5 GHz the exponent drops to 1.6. For the Main St. location, the exponent decreases with frequency from 3 at 700 MHz to 1.7 at 5 GHz. In the Main St. environment, the exponent 1.7 for the 5 GHz case makes sense due to waveguiding effects. The intercepts increase with frequency at both locations, as expected, increasing over approximately the same interval, about 48 dB at 700 MHz to about 73 dB at 5 GHz. The standard deviation also decreases similarly as frequency increases, starting at about 12.8 dB at 700 MHz to 6.7 dB at 5 GHz. The two ray (or in general, multipath) attenuation peaks contribute to the larger values of standard deviation.

For the Beltline location, antenna inside-car cases, the path loss exponent again increases from 700 to 2400 MHz, but drops below 2 for the 5 GHz case. At the Main St. location, the exponent decreases with frequency until reaching the lowest value for any

case, 1.1 at 5 GHz. This again might be due to waveguiding at the Main St. location. The intercept for the open Beltline environment increases with frequency as expected. The Beltline antenna inside-car intercepts increase from 59.1 dB at 700 MHz to 85.7 at 5 GHz, whereas the Main St. intercepts increase from 57.7 dB to 78.9 dB; the Main St. intercepts are in general smaller, as expected. Similarly, the Beltline inside-car standard deviations decrease from 12.7 dB at 700 MHz to 5.2 dB at 5 GHz. The Main St. standard deviations decrease from 10 dB at 700 MHz to 4.9 dB at 5 GHz.

The position of the antenna also affects the magnitude of the exponents at each location. The 700 MHz and 5 GHz cases show that, at both locations, the path loss exponent is smaller for the inside-car cases than the outside-car cases. This difference is small, about 0.3 for the 700 MHz cases at both locations and 0.6 for the 5 GHz cases at both locations. The 2.4 GHz cases yield an exponent only 0.1 greater for the antenna inside-car cases than the outside-car cases. As seen in the previous section the intercept points—which indicate gross attenuation at the minimum measured distance—are always larger for the antenna inside-car cases than the outside-car cases at every frequency and at both locations. The largest difference between these values is for the 5 GHz Beltline cases where the antenna outside-car intercept is 72.5 dB and the inside-car intercept is 85.7 dB: a 13.2 dB difference. The smallest is the 2.4 GHz Main St. cases where the outside-car intercept is 59.1 dB and the inside-car intercept is 62.3 dB, or a 3.2 dB difference.

Finally, the standard deviation follows a similar pattern to the path loss exponent. The 700 MHz and 5 GHz values are larger for the outside-car cases than the inside-car cases at both locations. The 2.4 GHz cases again show the reverse, where the inside-car cases have larger values than the outside-car values, although the standard deviation

decreases with frequency consistently for each antenna position and location. The largest standard deviation is the 13.1 dB of the 700 MHz Beltline location, outside-car case and the smallest is 4.9 dB of the 5 GHz Main St. location, inside-car case. Figure 4.20 shows the path loss exponents versus frequency for each case. From the figure it is easy to see how the path loss exponents are separated by location. The Beltline location typically has larger exponents than the Main St. location.

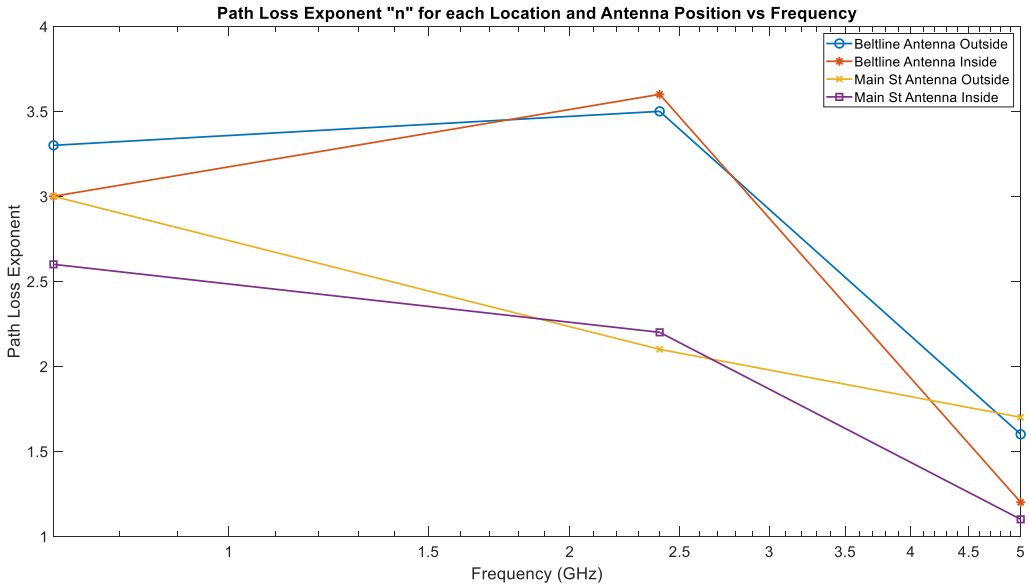

Figure 4.20. Path loss Exponent vs Distance for each Location and Antenna Position

Similarly, the standard deviations versus frequency for each case are shown in Figure 4.21. Again the Beltline location has larger values of standard deviation than the Main St. location and each antenna position has similar values for both locations. We thus observe that both path loss exponent and linear fit standard deviation tend to decrease as frequency increases.

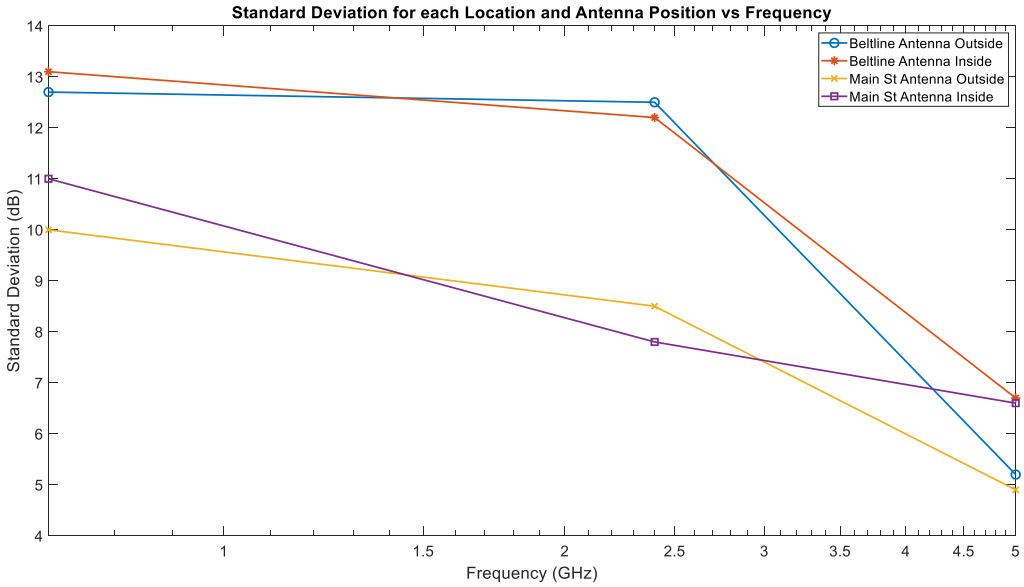

Figure 4.21. Standard Deviation vs. Distance for each Location and Antenna Position.

Chapter 5: Conclusion

In this thesis, we examine the effects of a low-height antenna on the path loss of a curb to vehicle channel. We start by reviewing the theory behind path loss and antenna gain patterns. Then we described the test procedure, the test environments, and the test equipment. Finally we discussed the results of the tests by comparing the fit parameters (path loss exponent, intercept, and the standard deviation of the averaged trials to the linear fit) for each frequency, antenna position and test location.

As stated in the previous chapter, the average difference between the average fit line and the 2-ray attenuation varies with antenna position and test location. The difference between the average fit line and the 2-ray attenuation is greater for the Beltline location than the Main St. location, and the inside-car antenna position has a higher attenuation than the outside-car position. The path loss exponents and standard deviations for each case tend to be closer for cases of the same location rather than antenna position. That is to say that the path loss exponents and standard deviations, for a given frequency and location, are closer in value than those of a different location, regardless of antenna position. This all implies that though the Beltline location is closer to a freespace environment since there are fewer objects for the signal to scatter or reflect from, the Main St. location is better suited for low-height antenna to vehicle propagation due to the addition of MPCs.

Future work would include repeating the test with a wideband test setup to provide a more accurate model of the channel, i.e., the channel's impulse response. Other test locations should also be included such as additional open areas, additional urban areas,

suburban settings, higher density urban (city environments with larger buildings and more traffic), and highways as well as NLOS tests in all these environments. Finally other antenna types should be used to help determine effective antennas for any potential curbside applications.

References

[1] D. W. Matolak, I. Sen and W. Xiong, "Channel Modeling for V2V Communications," *International Conference on Mobile and Ubiquitous Systems*, 17-21 July 2006.

[2] J. Karedal, N. Czink, A. Paier, F. Tufvesson and A. F. Molisch, "Pathloss Modeling for Vehicle-to-Vehicle Communications," *IEEE Transactions on Vehicular Technology*, vol. 60, no. 1, pp. 323-328, 2011.

[3] D. W. Matolak and Q. Wu, "Channel Models for V2V Communications: A Comparison of Different Approaches," in *Proceedings of the 5th European Conference on Antennas and Propagation*, Rome, 2011.

[4] C. Phillips, D. Sicker and D. Grunwald, "A Survey of Wireless Path Loss Prediction and Coverage Mapping Methods," *IEEE Communications Surveys & Tutorials*, vol. 15, no. 1, pp. 255-270, 2013.

[5] H. Nguyen and E. Shwedyk, A First Course In Digital Comunnications, New York: Cambridge University Press, 2009.

[6] C. Levis, J. Johnson and F. Teixeira, Radiowave Propagation, Hoboken, N.J.: John Wiley & Sons, 2010.

[7] A. Hugine, H. I. Volos, J. Gaeddert and R. M. Buehrer, "Meausrement and Characterizations of the Near-Ground Indoor Ultra Wideband Channel," in *IEEE Wireless Communications and Networking Conference*, Las Vagas, 2006.

[8] G. G. Joshi, C. B. Dietrich, C. R. Anderson, W. G. Newhall, W. A. Davis, J. Isaacs and G. Barnett, "Near-ground Channel Measurments over Line-of-Sight and Forested Paths," *IEEE Proceedings - Microwaves, Antennas and Propagation,* vol. 152, no. 6, pp. 589 - 596, 2005.

[9] C. Balanis, Antenna Theory - Analysis and Design, Hoboken: John Wiley & Sons, 2005.

[10] L-Com, "HyperLink Wireless Brand 4.9-5.8 GHz 6 dBi Omni-directional Antenna Model: HGV-4958-06U".

[11] RF Engineering, "4G Antenna_RFCA-Specification".

[12] W. Stutzman and G. Thiele, Antenna Theory and Design, Ney York: Wiley, 2013.

[13] E. J. Jaselskis, J. Grigas and A. Brilingas, "Dielectric Properties of Asphalt Pavement," *Journal of Materials In Civil Engineering,* vol. 15, no. 5, pp. 427-434, 2003.